

## Effect of Electron Parallel Compressibility on Collisionless MHD Modes

MATSUMOTO Taro, TOKUDA Shinji, KISHIMOTO Yasuaki and NAITOU Hiroshi<sup>1</sup>

*Naka Fusion Research Establishment, Japan Atomic Energy Research Institute, Naka, 311-0193, Japan*

<sup>1</sup>*Dep. of Electrical and Electronic Engineering, Yamaguchi Univ., Ube, 755-8611, Japan*

(Received: 11 December 2001 / Accepted: 9 May 2002)

### Abstract

The effect of the electron parallel compressibility (that is proportional to the ion sound Larmor radius) on the collisionless MHD modes is studied for  $\delta_e \geq \rho_s$  by the gyro-kinetic particle simulation. The growth rate before the internal collapse is found to be enhanced nonlinearly due to the electron parallel compressibility, although the linear growth is mediated by the electron inertia. As the electron skin depth decreases, the growth rate of the  $m = 1$  kink mode saturates by an geometrical effect which is independent of the microscopic scales.

### Keywords:

collisionless MHD mode,  $m=1$  internal kink, tokamak plasma, electron inertia, ion sound Larmor radius, parallel compressibility, magnetic reconnection, particle simulation

### 1. Introduction

In fusion plasma research, the tokamak type device has a great advantage for a candidate of commercial fusion reactor. In tokamaks with high current density where the safety factor at the magnetic axis is less than unity, the  $m = 1$  internal kink mode evolves and causes the internal collapse. In tokamaks with the reversed shear configuration, the high performance discharge is often suspended by the fast collapse as the minimum safety factor has just come down less than two. The time scale of these collapses is larger than the value predicted by the resistive MHD theory.

In the collisionless plasma with high temperature, the physics of the internal mode is affected by many elementary processes of plasma. In particular, the magnetic reconnection can be induced by the electron inertia and the electron parallel compressibility. The characteristic scale of length are the electron skin depth,  $\delta_e (= c/\omega_{pe})$ , and the ion sound Larmor radius (the ion Larmor radius measured with the electron temperature),

$\rho_s$ , respectively. Therefore, the nonlinear evolution of the internal modes should be analyzed with these collisionless effects.

The importance of the electron inertia for the  $m = 1$  mode is firstly pointed out by Wesson [1], and is included in the nonlinear simulation by Biskamp [2] and Naitou [3]. The effect of the electron parallel compressibility is studied with the linearized model by Porcelli [4], and is involved in the simulation for  $\rho_s \gg \delta_e$  by Aydemir [5]. The nonlinear behavior is qualitatively explained by Wang [6], although there is much scope to discuss in detail.

In this paper, we study the effect of the electron parallel compressibility on the collisionless internal mode in the region of  $\delta_e \geq \rho_s$  by the gyro-kinetic particle simulation. This paper is organized as follows. In Sec. 2, we described the simulation model and parameters briefly. In Sec. 3, the simulation results of the collisionless  $m = 1$  kink-tearing mode are shown. The

---

Corresponding author's e-mail: [tmatsumo@naka.jaeri.go.jp](mailto:tmatsumo@naka.jaeri.go.jp)

growth rate before the internal collapse is found to be enhanced nonlinearly due to the electron parallel compressibility, although the linear growth is mediated by the electron inertia. The results of the collisionless  $m = 2$  double tearing mode are also shown. Finally, a brief summary is given in Sec. 4.

## 2. Simulation Model and Parameters

In the gyro-kinetic model, plasma can be described with the equations which do not include any frequency higher than the ion cyclotron frequency, since the physical phenomena are averaged with respect to the ion Larmor radius by the gyro-kinetic ordering [7]. The gyro-kinetic model permits the time step much longer than the electron plasma frequency, and is appropriate to the analysis for the phenomena whose frequency is the same order of Alfvén frequency such as the collisionless internal kink mode.

The gyro-kinetic equations used in this simulation are the same to those in ref. 8. Each particle has the longitudinal generalized momentum individually, which is assumed to form a shifted Maxwellian for the initial equilibrium distribution. Then, the electron parallel compressibility and the electron inertia effects are included through the variation of the parallel momentum. The dynamics of particles are computed in a three dimensional rectangular box with the Cartesian coordinates  $(x, y, z)$ . Toroidal effects are ignored for simplicity. A periodic boundary condition is adopted in

the  $z$  direction, and a perfect conducting wall is imposed on the  $x$ - $y$  boundary surfaces. We choose safety factor profile that is 0.85 on the magnetic axis and unity near the half radius, as shown in Fig. 1. The main parameters are listed on Table 1. In the present simulation, we assume the uniform density and temperature profiles.

In this research, the parameter region is restricted to  $\delta_e \geq \rho_s$ . Then, the effect of the finite Larmor radius due to averaging the fields is ignored. However, the electron parallel compressibility proportional to the ion sound Larmor radius is included, which affects the nonlinear evolution of the collisionless modes as mentioned below.

## 3. Simulation Results

### 3.1 Linear growth rate of $m=1$ mode

At first, to study the effect of  $\delta_e$  for different  $\rho_s$ , the collisionless  $m = 1$  mode is simulated in the normal shear configuration, as shown in Fig. 1(a). Figure 2 shows the linear growth rates of the electrostatic potential energy. In each  $\rho_s$  case, the linear growth rate has  $(\delta_e / r_1)^1$  dependence, which qualitatively agrees with the analytical growth rate for the collisionless  $m = 1$  mode induced by the electron inertia [4]. Here,  $r_1$  is the radius of the  $q = 1$  resonant surface, and nearly the half of the plasma radius. On the other hand, the effect of the electron parallel compressibility is small because the linear growth rate has weak dependence for  $\rho_s$ . Therefore, it is found that the magnetic reconnection in  $\delta_e \geq \rho_s$  region is mainly mediated by the electron inertia.

Table 1 The main parameters in the simulation

System Size ( $L_x \times L_y \times L_z$ )	128 × 128 × 32
Number of Particles (for $i, e$ )	16,777,216
Thermal Velocity ( $V_A$ )	0.18~0.38
Electron Skin Depth ( $\delta_e/a$ )	0.047~0.188
Ion Sound Larmor Radius ( $\rho_s/a$ )	0.023~0.047
$\delta_e/\rho_s$	1.33~6.00

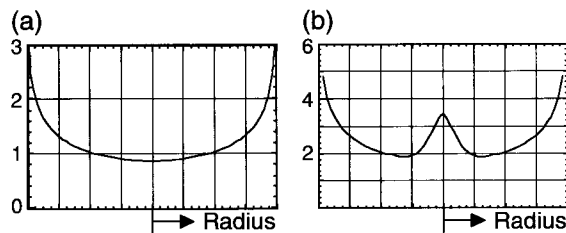


Fig. 1 Safety factor profiles for the simulations of (a) the  $m = 1$  kink-tearing mode and (b) the  $m = 2$  double tearing mode.

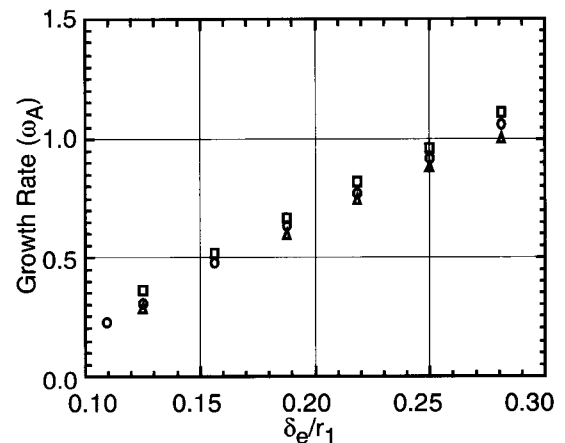


Fig. 2 The linear growth rate of the  $m = 1$  mode. The triangles, the circles and the squares denote  $\rho_s/r_1 = 0.0469, 0.0625$  and  $0.0938$ , respectively.

### 3.2 Nonlinear enhancement

However, the drastic change appears in the nonlinear behavior before the internal collapse. Figure 3 shows the time evolution of the growth rate of the electrostatic potential energy. In the case of  $\delta_e / r_1 = 0.312$ , the mode grows linearly till the collapse, since the collisionless width of the current sheet does not vary differently from the resistive width of the current sheet in the collisional plasma. On the other hand, as decreasing  $\delta_e$ , the growth rate is found to be enhanced nonlinearly. In particular, the behavior of the growth rate before the collapse is the same for  $\delta_e / r_1 \leq 0.156$ .

Figure 4 shows the maximum growth rate obtained just before collapse. It is clarified that the growth rate

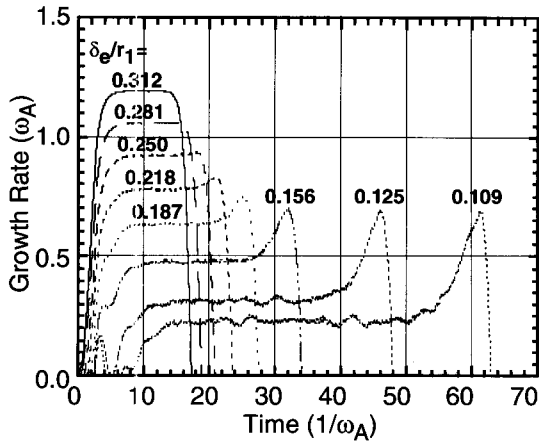


Fig. 3 Growth rate of the  $m = 1$  mode.  $\delta_e / r_1$  is changed between 0.109 and 0.312.  $\rho_s / r_1$  is fixed to 0.0625.

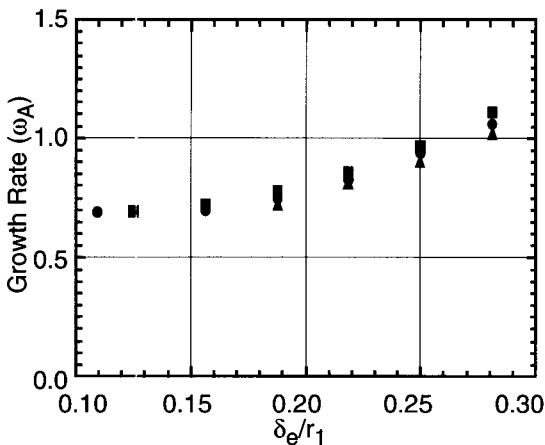


Fig. 4 The maximum growth rate of the  $m = 1$  mode. The triangles, the circles and the squares denote  $\rho_s / r_1 = 0.0469, 0.0625$  and  $0.0938$ , respectively.

saturates to be constant as  $\delta_e$  decreases. Comparing the growth rate of Fig. 4 with Fig. 2, the nonlinear enhancement of the growth rate is found to become larger as  $\delta_e$  decreases. Moreover, the saturation level is almost independent of  $\rho_s$ . Then, it is clarified that the nonlinear enhancement does not depend on the microscopic scales such as  $\delta_e$  and  $\rho_s$ .

### 3.3 Nonlinear Effect of $\rho_s$

In the absence of  $\rho_s$ , the potential flow in the vicinity of the reconnection point has a singularity, if X-type structure is formed. Then, the macroscopic current sheet is formed with Y-type structure [9]. The length of the current sheet,  $\Delta$ , is of order of  $r_1$ , while the width of the current sheet is  $\delta_e$  in the collisionless plasma. Therefore, from the pressure balance in the current sheet, the upstream velocity is described as  $U_0 = (\delta_e / \Delta) V_0$ , where  $U_0$  and  $V_0$  are the perpendicular velocity of the upstream inflow and the downstream outflow, respectively. When  $\delta_e / r_1 \ll 1$ ,  $U_0$  is much less than  $V_0$ , which is restricted to be less than  $V_A$ .

On the other hand,  $\rho_s$  has the smoothing effect for the potential flow around the reconnection point. Then, for finite  $\rho_s$ , the singularity disappears, and the current sheet with X-type structure can be formed. Therefore, as the plasma displacement increases, the angle of the outflow cone becomes broaden. The nonlinear enhancement of the growth rate corresponds to the acceleration of  $U_0$  due to the electron parallel compressibility. Figure 5 shows the Poincaré plots of the linear growing phase and the nonlinear evolving phase with the parameters of  $\delta_e / r_1 = 0.109$  and  $\rho_s / r_1 = 0.0625$ . It is confirmed that the angle of the outflow becomes broaden nonlinearly. It is also found that the core plasma is elongated in the moving direction, which is a characteristic of X-type reconnection.

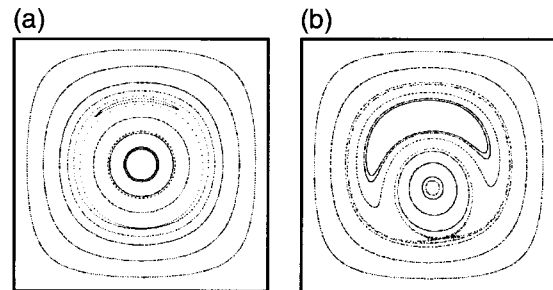


Fig. 5 Poincaré plots of the  $m = 1$  mode in (a) the linear growing phase ( $t \sim 31.65$ ) and (b) the nonlinear evolving phase ( $t \sim 57.48$ ).

### 3.4 $m=2$ Double tearing mode

The collisionless  $m = 2$  double tearing mode is also simulated in the reversed shear configuration, as shown in Fig. 1(b). Figure 6 shows the time evolution of the growth rate. As  $\delta_e$  decreases, the nonlinear enhancement is observed as well as the  $m = 1$  mode. However, the saturation level is not clear, because the coupling of two resonant surfaces is varied for finite displacement of plasma.

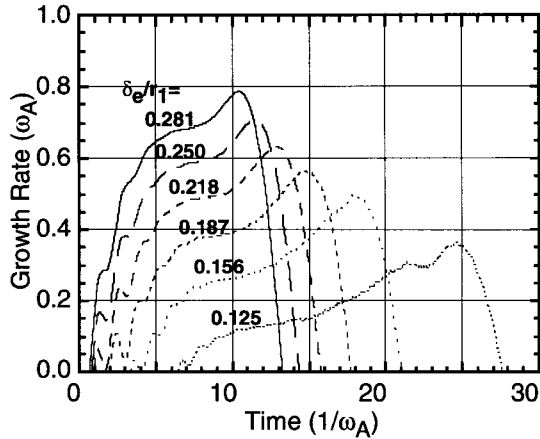


Fig. 6 Growth rate of the  $m = 2$  double tearing mode.  $\delta_e/r_1$  is changed between 0.125 and 0.281.  $\rho_s/r_1$  is fixed to 0.0625.

### 4. Discussion

The effect of the electron parallel compressibility, which is proportional to the ion sound Larmor radius, on the collisionless MHD modes is studied by the gyrokinetic particle simulation. The growth rate before the internal collapse is found to be enhanced nonlinearly due to the electron parallel compressibility, although the linear growth is mediated by the electron inertia. As the electron skin depth decreases, the growth rate of the  $m = 1$  mode saturates by an effect which is independent of the microscopic scales such as  $\delta_e$  and  $\rho_s$ .

Up to this research, the nonlinear effect of  $\rho_s$  is mainly discussed for  $\rho_s \gg \delta_e$  [5,6]. We have clarified that this nonlinear effect is also obtained for  $\rho_s \leq \delta_e$ .

The nonlinear enhancement is also obtained for the  $m = 2$  double tearing mode, although the saturation level is not obvious, because the coupling of two resonant surface is varied for finite plasma displacement.

### References

- [1] J.A. Wesson, Nucl. Fusion **30**, 2545 (1990).
- [2] D. Biskamp *et al.*, Phys. Rev. Lett. **73**, 971 (1994).
- [3] H. Naitou *et al.*, Phys. Plasmas **2**, 4257 (1995).
- [4] F. Porcelli, Phys. Rev. Lett. **66**, 425 (1991).
- [5] A.Y. Aydemir, Phys. Fluids **B4**, 3469 (1992).
- [6] X. Wang and A. Bhattacharjee, Phys. Rev. Lett. **70**, 1627 (1993).
- [7] W.W. Lee, Phys. Fluids **26**, 556 (1983).
- [8] T. Matsumoto *et al.*, J. Plasma and Fusion Res. **75**, 1188 (1999).
- [9] S.I. Syrovatskii, Sov. Phys. JETP **33**, 933 (1971).